8-2019

Airborne Characterization of Black Carbon Aerosol in California from Biomass Burning

Walt Williams
Clemson University, isaacwilliamsiii@gmail.com

AIRBORNE CHARACTERIZATION OF BLACK CARBON AEROSOL IN CALIFORNIA FROM BIOMASS BURNING

A Thesis

Presented to

the Graduate School of

Clemson University

In Partial Fulfillment

of the Requirements for the Degree

Master of Science

Environmental Engineering and Science

---

by

Walt Williams

August, 2019

Accepted by:

Dr. Andrew Metcalf, Committee Chair

Dr. David Freedman

Dr. David Ladner

Abstract

During the summer of 2018, the Clemson Air Quality Lab participated in the marine aerosol cloud and wildfire study (MACAWS), an aircraft-based field campaign in Monterey, CA. During this campaign, data was collected on atmospheric black carbon aerosol (BC) near the central coast of California. BC was evaluated from sources dominated by urban emissions, wildfires, and the offshore shipping industry. Data was collected on BC mass concentrations and size distribution using a single particle soot photometer (SP2). Additionally, an aerosol mass spectrometer (AMS) collected data on chemical composition of aerosols.

The hypothesis being tested was as follows: different sources of air pollution generate aerosol containing unique physical and chemical characteristics. Wildfires emit different characteristic black carbon aerosol size distributions and overall chemical compositions than other sources. These characteristics can be used to search for traces of biomass burning even within polluted air masses.

The purpose of this work is to increase overall understanding of ultrafine emissions from wildfires, especially black carbon particles. In order to test the hypothesis and contribute to this topic broader topic of wildfire air quality, the specific objectives are:

- Determine background mass concentrations of black carbon and other non-refractory species in the Sacramento Valley during fire season
- Investigate the size distribution of black carbon aerosol from wildfires
- Examine the emission of co-emitted aerosol from wildfires

- To use models and on board instruments to examine the plume dynamics in the atmosphere

The majority of the analysis has focused on measurements of two wildfires in the Sacramento Valley (SV). The first fire, the Pawnee Fire, did not produce enough emissions to generate widespread air quality effects. Instead, it represents a background aerosol concentration for fire season in the SV. The County Fire was the most prominent event during the campaign, burning 90,000 acres in early July, 2018. The direct plume contained an over 100 times more BC than background samples. This BC had a larger size distribution, consistent with those listed in literature from wildfires.

In addition to measuring the influence of the County Fire, several methods have been developed for estimating impact of future fires. One such technique used published emission factors (EF) to estimate various other chemical constituents emitted from a fire given a measured concentration of black carbon. When this technique was performed for the County Fire, emissions were estimated within a factor of 2 of measured values. Additionally, HYSPLIT models simulated the plume transportation from the fire location and were compared to the plume as described by the in-flight measurements.

The work performed herein validates the background air pollution data of prior sampling campaigns in the SV and displays a complete BC size distribution for an active wildfire. Additionally, new techniques are developed that allow scientists to estimate concentration of co-emitted aerosol from fires. Atmospheric dispersion models have also been performed and compared to in flight measurements, giving policy makers additional confidence in the accuracy of a key tool in environmental public health.

Acknowledgements

Special thanks goes to my advisor, Dr. Andrew Metcalf, whose unending patience and optimism has made this work possible. Each time I lost focus and became dejected, Dr. Metcalf was willing to help, whether it was with a short section of code or big picture questions about the direction of our research. To date, he has answered 487 emails and has never (openly) reconsidered his open door policy. His tireless work to fund his students, publish research, and teach good classes all while raising a young family is truly commendable.

Additional thanks to Taylor, who has made the transition from my girlfriend to fiancé to wife during our stay in South Carolina. She trusted my judgement and moved to a state neither of us had ever been to so I could pursue further education. She talked me out of quitting when I realized Bojangles cashiers were paid more than graduate students, and has patiently listened to me stress about deadlines while she assumed the lion's share of the work associated with planning a wedding. I hope to have the opportunity to repay some small portion of this debt while she finishes her thesis in the upcoming year.

Many others have also played a part in this thesis and also deserve recognition. Those include McKenna Dove, Camren Shea, and Robert Basha, the undergraduate researchers most closely associated with this work; Ali Mohammadi Nafchi and Nilima Sarwar, Dr. Metcalf's other graduate students; Connor Parker, Jessica Deaver, Joel Neuder, Colby Cash, and Paige Taber, the active members of our cohort; and Kathryn Peruski, the resident expert on grad school.

Table of Contents

List of Figures and Tables

Figure Page

Tables Page

List of Abbreviations

BC: Black Carbon Aerosol

SP2: Single Particle Soot Photometer

AMS: Aerosol Mass Spectrometer

RF: Research Flight

MMD: Mass Median Diameter

BB: Biomass Burning

$PM_{10, 2.5, 1}$: Mass of particulate matter smaller than 10, 2.5, and 1 μm in diameter, respectively

HYSPLIT: Hybrid Single Particle Lagrangian Integrated Trajectory Model

SV: Sacramento Valley

SMPS: Scanning Mobility Particle Sizer

SEMS: Scanning Electrical Mobility Sizer

CA: California

EPA: environmental protection agency

WHO: World Health Organization

NPS: Naval Postgraduate School

CALNEX: California Nexus, Research at the Nexus of Climate Chang and Air Quality

FLAME: Fire Laboratory at Missoula Experiments

MACAWS: Marine Aerosol Cloud and Wildfire Study

IPCC: Intergovernmental Panel on Climate Change

CIRPAS: Center for Interdisciplinary Remotely Piloted Aircraft Studies

PSAP: Particle Soot Absorption Photometer

CPC: Condensation Particle Counter

UFCPC: Ultrafine Condensation Particle Counter

PSL: Polystyrene Latex Spheres

Introduction

Research Overview

Hypothesis

Different sources of air pollution generate aerosol containing unique physical and chemical characteristics. Wildfires emit different characteristic black carbon aerosol size distributions and overall chemical compositions than other sources. These characteristics can be used to search for traces of biomass burning even within polluted air masses.

Objectives

The purpose of this work is to increase overall understanding of ultrafine emissions from wildfires, especially black carbon particles. In order to contribute to this broader topic, the specific objectives are:

- Determine background mass concentrations of black carbon and other non-refractory species in the Sacramento Valley during fire season
- Investigate the size distribution of black carbon aerosol from wildfires
- Examine the emission of co-emitted aerosol from wildfires
- To use models and on-board instruments to examine the plume dynamics in the atmosphere

Black Carbon

Black carbon aerosol (BC) is a component of smoke, and is generated anywhere incomplete combustion takes place. Although BC occupies a small fraction of smoke by mass, it can have serious effects on the environment and human health (Highwood & Kinnersley, 2006). BC is the second most important anthropogenic emission in terms of its climate forcing in the

present-day atmosphere; only CO_2 is estimated to have a greater forcing (Bond et al., 2013). Moreover, combustion-derived particulate matter is a potent contributor to human health effects (Mills et al., 2009). These findings, along with recent advances in measurement technology, have stimulated an increase in research into a wide variety of topics concerning BC and other combustion-generated particles (e.g. Bond et al., 2013; Fawole et al., 2016; Gertler et al., 2016; Janssen et al., 2012).

BC can be differentiated from other similar combustion-generated particles, including refractory black carbon, brown carbon, graphitic carbon, elemental carbon, and light absorbing carbon. The definition of BC considered here follows that proposed by Bond et al. (2013); it strongly absorbs light at all visible wavelengths (Bond & Bergstrom, 2006) and is refractory and retains its basic form until temperatures reach ~4000 K (Schwarz et al., 2006). BC is generated by any source of incomplete combustion, including open biomass burning, diesel engines, industrial energy generation, aircraft emissions, and residential solid fuel burning; the largest worldwide source is open biomass burning (BB) (Bond et al., 2013; Bond et al., 2004). Because most of these sources are decentralized and difficult to measure, uncertainty exists in annual, worldwide BC generation and emissions. For example, the IPCC reported 13 million tons per year emitted in 2001 (Boucher et al., 2013), while Bond et al. (2013) reported 8.3 million tons for the year 2000 (while acknowledging an uncertainty range of 2.2 to 30 million tons). Emissions of BC are removed by a variety of processes, including wet removal and gravitational settling (Highwood & Kinnersley, 2006; Taylor et al., 2014). Wet deposition is the dominant mechanism and is key in determining the atmospheric lifetime and extent of global transport of BC (May et al., 2014; Taylor et al., 2014). These removal processes are poorly understood,

limiting the ability to quantify environmental effects. Several studies (May et al., 2014; Moteki et al., 2012; Taylor et al., 2014) indicate that particles with larger diameters and thick coatings of secondary species are preferentially removed by precipitation. The removal of such particles leaves smaller, more thinly coated particles behind. Considering all removal pathways, BC has an atmospheric lifetime on the order of a week (compared to 20- 200 years for CO_2 and hours to days for PM_{10}) (Archer et al., 2009; Demuzere et al., 2009; Venkatesh et al., 2011).

Because of the relatively short atmospheric lifetime of BC, its concentrations are highly localized. On large scales, BC is very inhomogeneous. For example, Shanghai has an annual average of 2.8-3.0 $\mu g/m^3$ BC (Feng et al., 2009) while the west coast of Ireland reported an annual average of 27.5 ng/m^3 (Kleefeld et al., 2002). Nonetheless, due to global transport, even environments such as the remote Arctic exhibit measurable concentrations of BC (McConnell et al., 2007). BC concentration gradients also exist on small scales due to proximity of a source. Roorda-Knape et al. (2002) reported that BC concentration dropped by 50% by mass within the first 300 m of a roadway (Janssen et al., 2012). Similar results have been found with other BC point sources such as power generation facilities and harbors (Lu et al., 2006; Polidori et al., 2010). In addition to variation in concentration, BC also varies in particle size. The characteristic size distribution of BC particles is determined by the combustion source of those particles (Table 1). The focus of this thesis is on BC generated by wildfires or open biomass burning (BB). Even within this category, there is considerable variation in particle size, as shown in Table 1. This variation is due to the complexity of combustion conditions, including combustion type, fire intensity, and combustion efficiency (Reid, et al, 2004).

Table 1**:** BC mass median diameter (MMD) reported elsewhere in literature.

Particle Source	BC MMD (nm)	Reference
BB (long range transport)	120-160	Dahlkötter et al. 2014
BB (Asia)	177-197	Kondo et al. 2011
BB (Canada)	176-238	Kondo et al. 2011
BB (California)	177-209	Sahu et al. 2012
BB (Texas)	200-220	Schwarz et al. 2008
BB (Canada)	195	Taylor et al. 2014
BB (Wyoming)	170	Pratt et al. 2011
Urban Emissions (California)	120-160	Metcalf et al. 2012
Urban Emissions (Texas)	160-180	Schwarz et al. 2008

California Wildfires and Air Quality

In 2003, a single wildfire near San Diego caused ambient sub-2.5 micron particulate matter ($PM_{2.5}$) concentrations in the city to increase to 170 $\mu g/m^3$, nearly three times the federal 24-hour average standard (Viswanathan et al., 2012). Moreover, wildfire activity in California and the rest of the western United States, in general, has increased in recent years, as shown in Figure 1 (Westerling et al., 2006). In 2018, wildfires in California burned 876,146 acres of land (Figure 1), the highest in recorded history going back to 1933 (CalFire, 2019). If it is assumed that most of this burning occurred in the state's dry chaparrals, which emit 1.3 g BC/kg fuel (Akagi et al., 2011; Merlet & Andreae, 2001) with a biomass loading of 50 Mg/ha and fuel fraction of 50% (Regelbrugge & Conard, 1998), approximately 12 Gg of BC were released into the atmosphere in California in 2018.

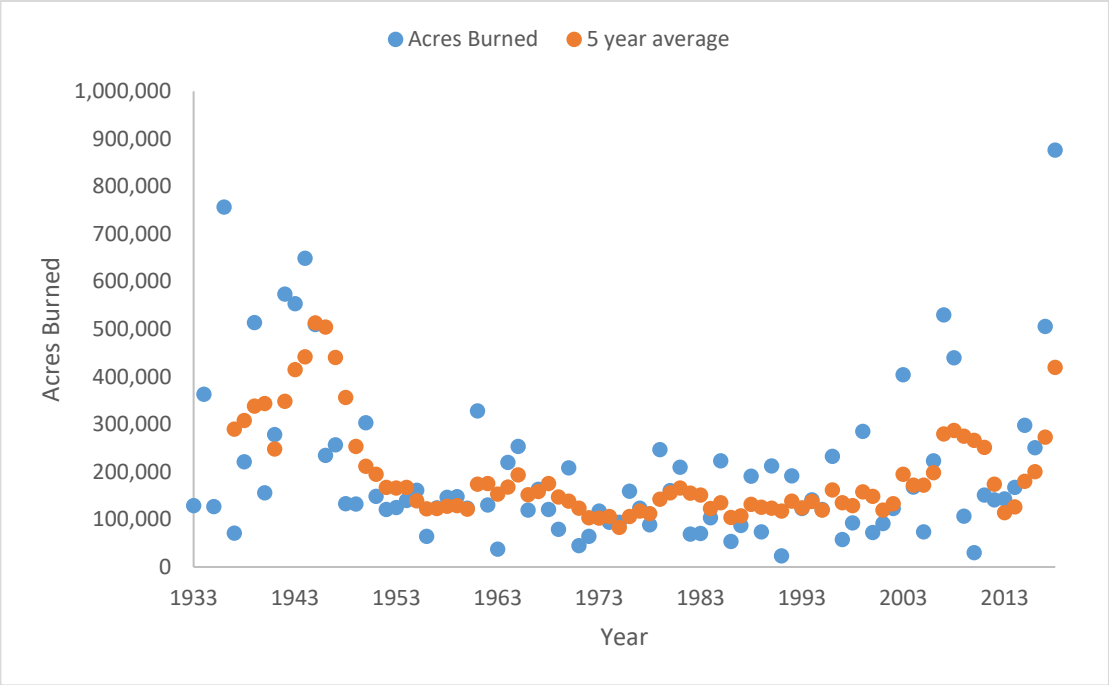

Figure 1: Acres burned in California by year (CalFire, 2019).

Even conservative estimates of climate change (Boucher et al., 2013) indicate an increase in California wildfire activity. Westerling and Bryant (2007) predicted a 20% increase in California wildfire likelihood by 2099, depending on location, and Fried et al. (2004) estimated a 41% increase in area burned for most of northern California. Since BC is a regional pollutant, this has drastic regional air quality implications for California's 40 million citizens.

Air Quality Impacts on Human Health

Ambient particulate matter (PM) has major impacts on human health. Generally speaking, total daily mortality increases by approximately 1% per 10 $\mu g/m^3$ increase in PM_{10} concentration (Harrison, 2000). This approximation depends on many factors, such as shape, particle size distribution, sulfate content, and trace element content. These factors will be addressed as they relate to combustion generated particle matter. Combustion generated particulate matter is the classification of particles that includes BC as well as any co-emitted

aerosols from a combustion source. Those studying health effects refer to combustion generated particulate matter generally instead of BC specifically because it is not necessary to separate the health effects of co-emitted species. These combustion-generated particles primarily occupy the ultrafine (PM_1, aerodynamic diameter smaller than 1 micron) size range and are composed of aromatic hydrocarbons, with potential coatings of sulfate, nitrate, and organic compounds.

The EPA and World Health Organization (WHO) both use mass concentration [$\mu g/m^3$] of $PM_{2.5}$ and PM_{10} as metrics for air quality. Since these are cumulative measurements, they include the entire size spectrum of combustion generated particles. However, not all particulate in those size ranges contributes equally to adverse health effects (WHO, 2007). The importance of particle composition was illustrated by Mills el al. (2008) by exposing a group of people to high concentrations of $PM_{2.5}$ composed of 90% sea salt and observing minimal health effects. Meanwhile, exhaust streams high in BC from diesel engine exhaust (Barath et al., 2010) and biomass combustion (Solomon et al., 2003) induced airway inflammation and impaired vascular function in human exposure tests even in dilute concentrations. Mills et al. (2009) indicated that combustion derived particulate matter is the most potent component of the air pollution cocktail. It remains unclear what portion of this increased toxicity is due to the small size of the particles, their potential for sulfate coatings, their chemical composition, or an additive effect from each.

The small size of BC particles limits the inertial forces the particles carry and prevents them from being removed by impaction in the upper airways. Further down the respiratory

tract, ultrafine particles penetrate deep into the alveoli before being deposited and causing oxidative stress to epithelial cells as shown in Figure 2 (Kennedy, 2007; Mills et al., 2009).

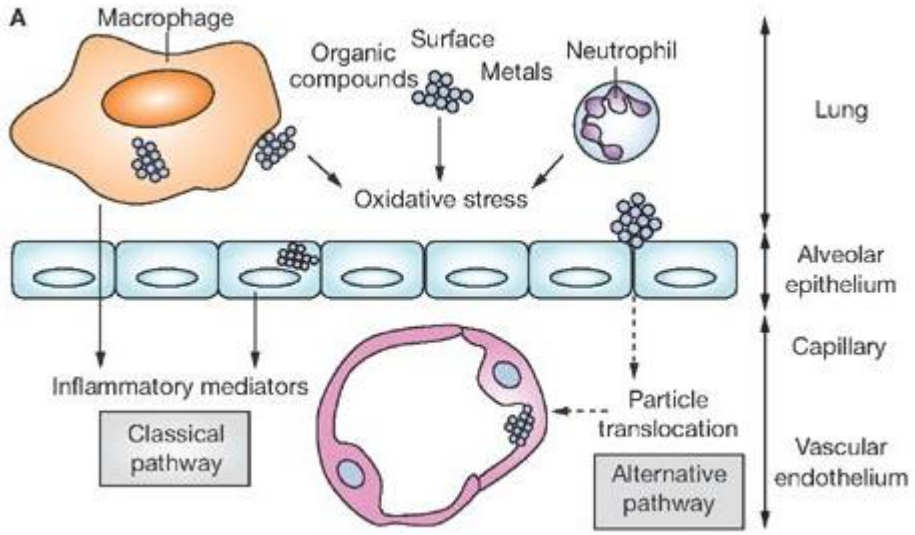

Figure 2: Pathways through which combustion derived particulate matter induces cardiovascular effects (adapted from Mills et al., 2009)

Combustion derived particulate matter presents two types of health effects. The first are indirect pulmonary effects, caused by the particles inducing oxidative stress and provoking an inflammatory response in the lungs, as shown in the classical pathway in Figure 2. The second, shown as the alternative pathway in Figure 2, involves these particles crossing from the lungs into the circulatory system where it can be lodged in organs such as the liver, spleen, and heart (Mills et al., 2009; Oberdörster et al., 2005). This process happens quickly and regularly; Nemmar et al. (2001) found that 25-30% of particles less than 80 nm were detected in the blood stream within 5 minutes of inhalation. Given BC's composition including a variety of dangerous

substances, such as 1, 3 butadiene (Penn et al., 2005), there is a clear risk associated with these particles travel through the blood stream.

Particulate matter presents a well-documented health risk, however, not all PM contributes equally to this risk. Combustion generated particulate matter, including BC, present a clear and present danger to human health even when present at small concentrations. This is the cause for concern when examining trends in increased wildfire activity in a densely populated area and is a portion of the justification for BC research.

Black Carbon and its Effects on the Environment

Human health is not the only factor motivating research on BC. It also carries significant weight as an agent of global warming due to its absorption of solar radiation. The magnitude of a global warming agent is quantifiable as radiative forcing, measured in watts per square meter. A positive radiative forcing indicates more energy reaching or remaining in earth's atmosphere, and leads to a warming effect. A negative radiative forcing indicates that less energy reaches the atmosphere, or that more energy leaves it, leading to a cooling effect. Bond estimates that BC is the second most important human emission in terms of its climate forcing in the present-day atmosphere, second only to CO_2 (Bond et al., 2013). However, the degree to which BC warms the atmosphere is uncertain- various models list heating values from 0.03 W/m^2 to 0.8 W/m^2 (Samset et al., 2014; Myhre et al., 2013). The Intergovernmental Panel on Climate Change (IPCC) lists two median values of 0.2 and 0.4 W/m^2 (IPCC, 2013). For reference, CO_2 has a radiative forcing of 1.62 $W/m^2 \pm 0.2$ (Boucher et al., 2013).

One reason BC has such large uncertainty in its climate effects is the complexity of its interactions with the atmosphere. As noted earlier, it is spatially inhomogeneous and difficult to

model transportation due to complex precipitation-based removal mechanisms. Additionally, aerosols affect the atmosphere differently than gases. There are four categories by which BC affects climate; each is detailed below, and an effort is made to quantify the radiative forcing due to this mechanism.

1) *Direct effects* are those caused by BC particles absorbing incoming solar radiation. This absorption heats the atmosphere where the particles are present and reduces the sunlight that reaches the surface of the earth (Bond et al., 2013). The range of estimates of radiative forcing has been cited as low as +0.1 W/m^2 (Penner et al., 2003) and as high as +1.26 W/m^2 (Bond et al., 2013 and references therein). The median value used in Bond et al. (2013) is given as +0.71 W/m^2.
2) *Indirect effects* involve BC's interaction with cloud formation. Indirect effects consist of nucleated or scavenged BC particles that alter the microphysics of clouds, changing droplet size, ice particle number, and cloud extent (Bond et al., 2013; Highwood & Kinnersley, 2006).
3) *Semi-direct effects* are a continuation of direct effects. As the atmosphere heats around BC particles, it alters atmospheric temperature profiles, which dictate cloud droplet size distributions. Indirect and semi-direct effects are frequently lumped together, and their climate forcing is variable based on region and highly uncertain, with estimates ranging from -0.61 W/m^2 to 1.0 W/m^2 (Bond et al., 2013, and references therein).
4) *Surface albedo effects* mostly pertain to BC that has been deposited on snow and ice. The presence of these light absorbing particles reduces the surface albedo and can lead to melting of the ice. The forcing is unanimously positive, and ranges from 0.04 W/m^2 to 0.33 W/m^2 (Bond et al., 2013, and references therein).

BC is a complex issue that is poorly understood. As described above, it has the potential to effect immediate human health and long-term climate. BC is generated in large metropolitan areas by fossil fuel combustion and near them by biomass burning, specifically wildfires. These wildfires are projected to increase in frequency and severity in the future, a positive feedback loop created in part by the emission of BC. Meanwhile, the estimates of global emission of BC into the atmosphere have error bars that extend over an order of magnitude and the radiative forcing is even less certain. Additionally, health effects are broad and poorly understood as well. These unanswered questions justify additional research into a broad range of BC topics. The portion of these topics addressed herein attempts to better understand the quantity and type of BC emitted from wildfires and begins to set up a framework for estimating co-emitted aerosols.

Methods

Mission Overview

The Marine Aerosol Cloud and Wildfire Study (MACAWS) was an aircraft-based field campaign originating from Marina, California in June and July 2018. The Naval Postgraduate School (NPS) Twin Otter was employed to carry out 16 research flights between June 15 and July 15, 2018. These flights are summarized in Figure 3. Each flight was given one of three designations: wildfire, ship tracking, or clouds/clear depending on the goals of that flight. Wildfire and ship tracking flights flew upwind of the source to sample background conditions, followed by a series of downwind and crosswind patterns to assess the nature of the plume. The wildfire and ship tracking flights also included tight spirals from low to high to low elevation (or the inverse) known as soundings to characterize vertical distribution of the plume. Since multiple vertical soundings in close proximity can lead to engine exhaust interference, only the first sounding in an area has been analyzed. Clouds/clear flights consisted of flying at a constant heading and altitude away from the coast of California, providing an excellent opportunity to characterize the transition from urban to clean marine environment, as well as sample clouds for cloud water content.

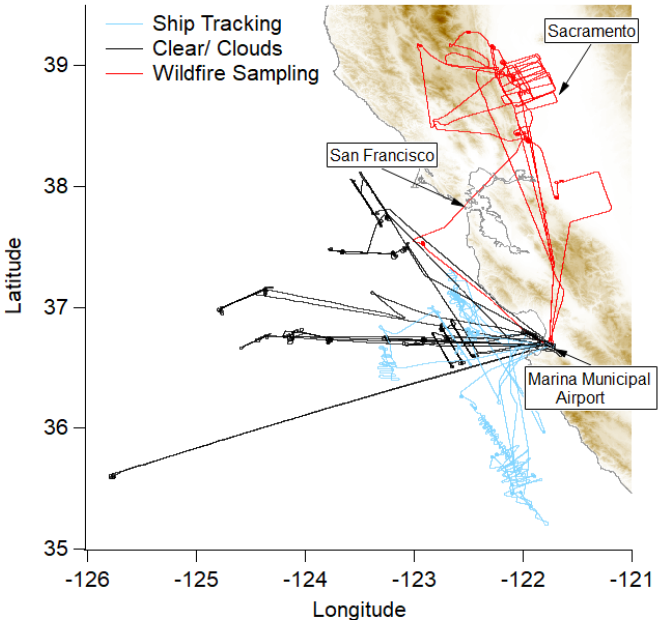

General Flight Information		
RF	**Flight Date**	**Mission Type**
1	6/21/2018	Ship Tracking
2	6/22/2018	Clouds/ Clear
3	6/25/2018	Ship Tracking
4	6/26/2018	Clouds/ Clear
5	6/27/2018	Clouds/ Clear
6a/b	6/28/2018	Pawnee Fire
7	6/29/2018	Ship Tracking
8	6/29/2018	Pawnee Fire
9	7/2/2018	Clouds/ Clear
10	7/3/2018	Clouds/ Clear
11	7/3/2018	County Fire
12	7/5/2018	Ship Tracking
13	7/6/2018	Ship Tracking
14	7/10/2018	Clouds/ Clear
15	7/11/2018	Ship Tracking
16	7/12/2018	Clouds/ Clear

Figure 3: *Left:* All flight paths during MACAWS, each flight starting from Marina Municipal Airport. *Right:* List of each flight and mission type. Research flights (RF) occurring on the same day were either split into separate numbers or designated with letters.

Instruments

The Twin Otter was outfitted with a suite of instruments capable of measuring aerosol particle size and number distribution, optical properties, and composition as detailed in Table 2. Each instrument pulled flow from a shared inlet. The inlet has a transmission efficiency near unity for particles smaller than 3.5 µm, indicating that all particles of relevant size ranges will be sampled without bias from the inlet (Hegg et al., 2005). The Twin Otter samples at approximately 50 m/s, allowing the flight pattern to be dictated by real time data.

Table 2: List of aerosol measurement equipment onboard the Twin Otter.

Instrument	Measurement	Aerosol Size Range	Uncertainty	Reference
Single Particle Soot Photometer (SP2)	Single particle BC mass	80 nm - 650 nm	±10%	(Moteki et al., 2007; Moteki et al., 2010)
	Single particle optical diameter of light scattering particles	200 nm - 350 nm	±30%	
Aerosol Mass Spectrometer (AMS)	Sub-micron, non-refractory bulk aerosol chemical composition	<1 µm	±35%	(DeCarlo et al., 2008; DeCarlo et al., 2006)
Condensation Particle Counters (CPC & UFCPC)	Number concentration of total particles	>30 nm (CPC) >4 nm (UFCPC)		
Particle Soot Absorption Photometer (PSAP)	Aerosol light absorption	N/A	±20%	(Sharma et al., 2017)
Nephelometer	Aerosol light scattering	N/A	±7%	(Anderson et al., 1996; Bond et al., 1999)

Single Particle Soot Photometer (SP2)

Data were collected on BC aerosol mass and number concentration and size distributions by a Single Particle Soot Photometer (SP2, Droplet Measurement Technologies, Boulder, CO, USA). The SP2 is a laser light-scattering and laser-induced incandescence measurement technique that allows for the simultaneous measurement of refractory BC mass and mixing state of single particles (Baumgardner et al., 2004; Schwarz et al., 2006; Stephens at al., 2003). The SP2 detects refractory black carbon mass by measuring the incandescence signal emitted from single BC-containing particles heated to their boiling point when passing through

an intense Nd:YAG laser beam (λ = 1064nm). The Clemson SP2 has been calibrated between 70 and 625 nm; only 4% of BC mass is under the lower size limit (Sahu et al., 2012). Atmospheric BC has a MMD between 140 and 210 nm (Table 1), so the distributions measured in the MACAWS campaign were well characterized by the SP2. Simultaneously, scattering signals are used to optically size single particles between 140 nm to 350 nm. Two incandescence detectors have different wavelength filters (broadband and narrowband) to assess the ratio of signals (dust will incandesce at a different wavelength ratio than refractory BC; thus, BC can be specifically identified). Two scattering detectors differ from each other as well: one detector is uniformly open while the second is a split detector to determine the location of each particle in the laser beam. Single particle data are saved during flights for offline analysis. Industry standards were followed (Laborde et al., 2012; Schwarz et al., 2010) to calibrate the Clemson SP2, details of which are presented in the following section. Moteki et al. (2007) estimated the uncertainty of determining diameter of BC particles using this method to be 13%, mostly due to scattering of the distribution of incandescence intensity for mono-dispersed BC.

SP2 Calibration

The SP2 was calibrated at the beginning of the field campaign and the scattering calibration was checked for drift before each flight. The broad and narrow band incandescence channels were calibrated using fullerene soot from Alfa Aesar (stock #40971, lot #FS12S011). The soot is no longer commercially available and was supplied by the NOAA Earth Science Research Lab (personal communication, Shuka Schwarz, 2018). This calibrant was chosen because it produces a similar ratio of particle mass to incandescence as atmospheric BC (Laborde, 2012), assuming a density of 1800 kg/m^3. DMT supplied Aquadag and 5-8% fullerene were also tested as possible calibration standards. As shown in Figure 4, the choice of standard

can make a difference of a factor of two in peak height per mass. Regardless of calibrant, the agreement between high and low gain within the detector is quite good. As a result, 13 particle sizes were selected between 80 nm and 625 nm, using the middle values to compare the gain settings, and the outer values to increase instrument range, as shown in Figure 4.

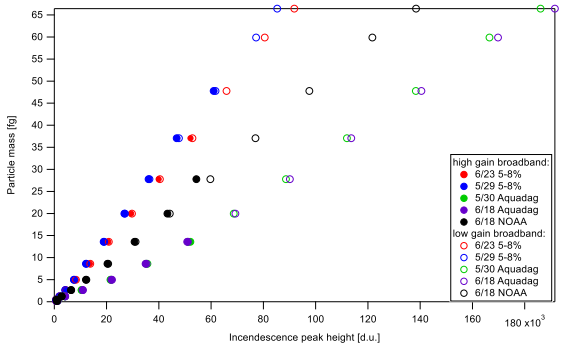

Figure 4: Broadband calibration curve.

Both the split and scattering detectors were calibrated with five sizes of certified polystyrene latex spheres (PSL; refractive index =1.59) ranging from 200 to 350 nm. Unfortunately, no split data is available for the MACAWS campaign due to detector malfunction. The open scattering detector was used to check laser power daily using 269 nm PSL spheres as

shown in Figure 5. YAG laser power was recorded to monitor its effect on PSL peak height, which appears insignificant.

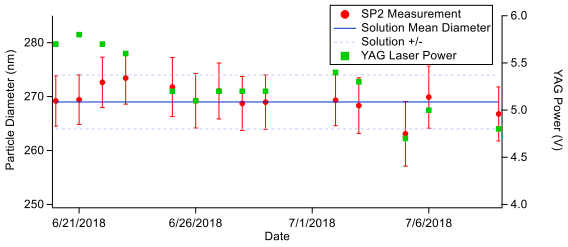

Figure 5: Monitoring 269 nm PSL over the duration of the campaign to check for drift in laser power. Error bars represent the log-normal distribution's width at half the maximum peak height.

HYSPLIT

The Hybrid Single Particle Lagrangian Integrated Trajectory Model (HYSPLIT) is commonly used in back trajectory calculations to find the source of an air mass (Dahlkötter et al., 2014; Feng et al., 2009; Gertler et al., 2016; Sedlacek et al., 2012; Taylor et al., 2014). This is a useful tool, allowing scientists to estimate potential for prior pollution in an air mass if the main back trajectory passed over a wildfire, through an urban area, or over an industrial area. Alternatively, it can be matched with weather forecasting to determine the for prior scavenging by precipitation events that may have altered the composition of a polluted air mass (Taylor et al., 2014). The back trajectories for the flights described here will predominantly indicate clean marine aerosol as the source of air masses prior to their intersecting with the event of interest. HYSPLIT has been used in a different context here than the previous studies. The model has

been used to generate forward trajectories emanating from the site of the fires. The model uses a source term and atmospheric measurements to determine the trajectory of the plume. The model output is polygons of equal concentration, spaced logarithmically, which can be manipulated in ArcMap. HYSPLIT has not been used in previous field campaigns in this manner and presents a powerful tool for those looking to forecast plumes from wildfires.

Aerosol Mass Spectrometer (AMS)

Aerosol chemical composition was measured using a high-resolution time-of-flight aerosol mass spectrometer (HR-ToF-AMS, Aerodyne Research Inc., hereafter referred to as AMS) (DeCarlo et al., 2006). Incoming air enters the AMS through a 100 μm critical orifice, after which an aerodynamic lens produces a particle beam that is accelerated under high vacuum. The particle beam is flash-vaporized on a resistively heated surface (600°C), and the resulting gases are ionized by electron impaction (70 eV). Individual ion identity is determined using a high-resolution time-of-flight mass spectrometer. Data were collected in V-mode, which has higher sensitivity but lower resolution than the alternative W-mode (due to a shorter path length within the mass spectrometer). The ionization efficiency (IE) of the AMS was calibrated before each flight. Data were averaged over 20 s intervals, and all data were analyzed using standard AMS software (SQUIRREL v1.57 and PIKA v1.16l) within Igor Pro 6.37. The collection efficiency (CE) was determined using the composition-dependent calculator within the SQUIRREL and PIKA software packages (Middlebrook et al., 2012).

Scanning Mobility Particle Sizer (SMPS)

Aerosol particle size distributions were measured by two SMPS's- Caltech's custom built SMPS and Clemson's Scanning Electrical Mobility Spectrometer (SEMS, Brechtel, Hayward, CA). The two instruments were set to scan different sizes, and the overlap has been used for

intercomparison between the instruments to demonstrate agreement and compare inversion techniques. Only SEMS data on particle mobility diameter will be displayed here. For the research flights presented here, the instrument scanned over 45 exponentially spaced bins from 100 to 1790 nm over a period of 70 s. The SEMS operated with a sheath to sample flow ratio of 5 (3:0.72 lpm) and a max voltage of 6,000 V. A mixing condensation particle counter (mCPC, Brechtel, Haywood, CA) with butanol as the working fluid is used in the Clemson SEMS. The calibration of SMPS can be checked by scanning over the size distribution of PSL particles of a known diameter.

Particle Soot Absorption Photometer (PSAP)

A Particle Soot Absorption Photometer (PSAP) is a three-wavelength measuring instrument that uses a filter-based method to measure aerosol light absorption aloft. The PSAP uses a filter to sample ambient air and an optical source and detector to determine the filter transmittance due to particulate matter (Arnott et al., 2006). Absorption techniques are not specific for BC, multiple other light-absorbing aerosol particles can be detected if measured at the wavelength (Bond et al., 2013). Scattering coefficients are needed to correct for the PSAP's filter transmission measurements and are determined using a nephelometer, which was also present onboard the Twin Otter (Arnott et al., 2006). Using an empirical value of MACBC of 7.5 +/- 1.2 m^2/g (Bond & Bergstrom, 2006; Clarke et al., 2004) and taking the average BC mass concentration of RF 11 (0.93 $\mu g/m^3$), the measured PSAP value reported as 6.98 Mm^{-1}, since the PSAP measurements held a relatively straight line at ~7 Mm^{-1}, it is assumed that this is noise generated from the instrument and that the PSAP failed to measure anything useful above this noise range.

Results and Discussion

County Fire

The County Fire was ignited on June 30, 2018 near Lake Berryessa by an improperly installed electric livestock fence (CalFire, 2019). By mid-July, the fire was fully contained at its maximum size of 90,288 acres. The area burned consisted primarily of blue oak woodland (DOI, 1998). These woodlands range from scattered islands of trees with a dominant understory of annual grasses and shrubbery, including poison-oak, California coffeeberry, and several species of ceanothus and manzanita, to a nearly closed canopy of primarily blue oak (*Final Management Plan for the Lake Berryessa Wildlife Area*, 1998). RF 11 sampled the County Fire while the fire was still actively flaming.

Figure 6 shows the flight path of RF 11 colored by the BC mass concentration as measured by the SP2. Several key observations can be made. First, it appears that we sampled a plume of BC aerosol on both the north and south sides of the County Fire. On the north side, the max BC mass concentration was 19.4 ug/m3 and the plume measured 10.4 km wide. On the south side, the max BC mass concentration was 19.4 ug/m3 and the plume measured 20.2 km wide, however the plume boundary was not as distinct as on the northern side of the County Fire. HYSPLIT model results show that the majority of the plume should have been advected towards the north during the sampling period of RF 11. The existence of southern plume is owing to the complex topography in the region and the fact that the flight restrictions did not totally preclude us from sampling over regions of active burning.

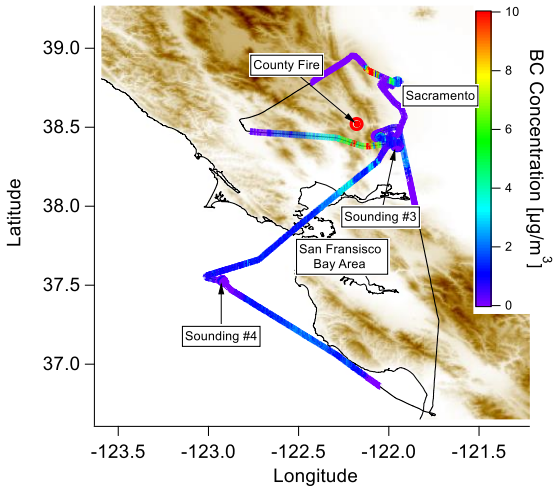

Figure 6: Flight path of RF 11, colored by BC mass concentration. Thin black lines indicate the flight track while the SP2 was off.

A HYSPLIT model was generated for the affected area starting July 2 at 6:00 PM and ending July 6 at 1:00 PM, the model contained the area covered in by the flight was run over the time the flight took place. The HYSPLIT trajectories shown in Figure 7 indicate the extent to which the fire affects air quality for northern California. The model was run at 500 m altitude

steps but failed to converge on a solution for the 1000- 1500 m interval. Because the model relies on archived weather data, it is unlikely this could be fixed retroactively. The results of the model are intended to describe the direction of the plume and relative concentration, not absolute concentration. The source was a 1 kg emission over the 12 hours prior to the flight. Potential future models could attempt to recreate the County Fire by describing the source as an area and estimating particulate matter emissions from the fire. The figure indicates the fire transporting the plume west into the Sacramento Valley before turning north once reaching the Sierra Nevada mountain range that confines the valley on the west. As altitude increases, the plume spreads out and begins to move south as altitude increases. The model fits measured results poorly and fails to locate the two hot spots north and south of the fire shown in Figure 6.

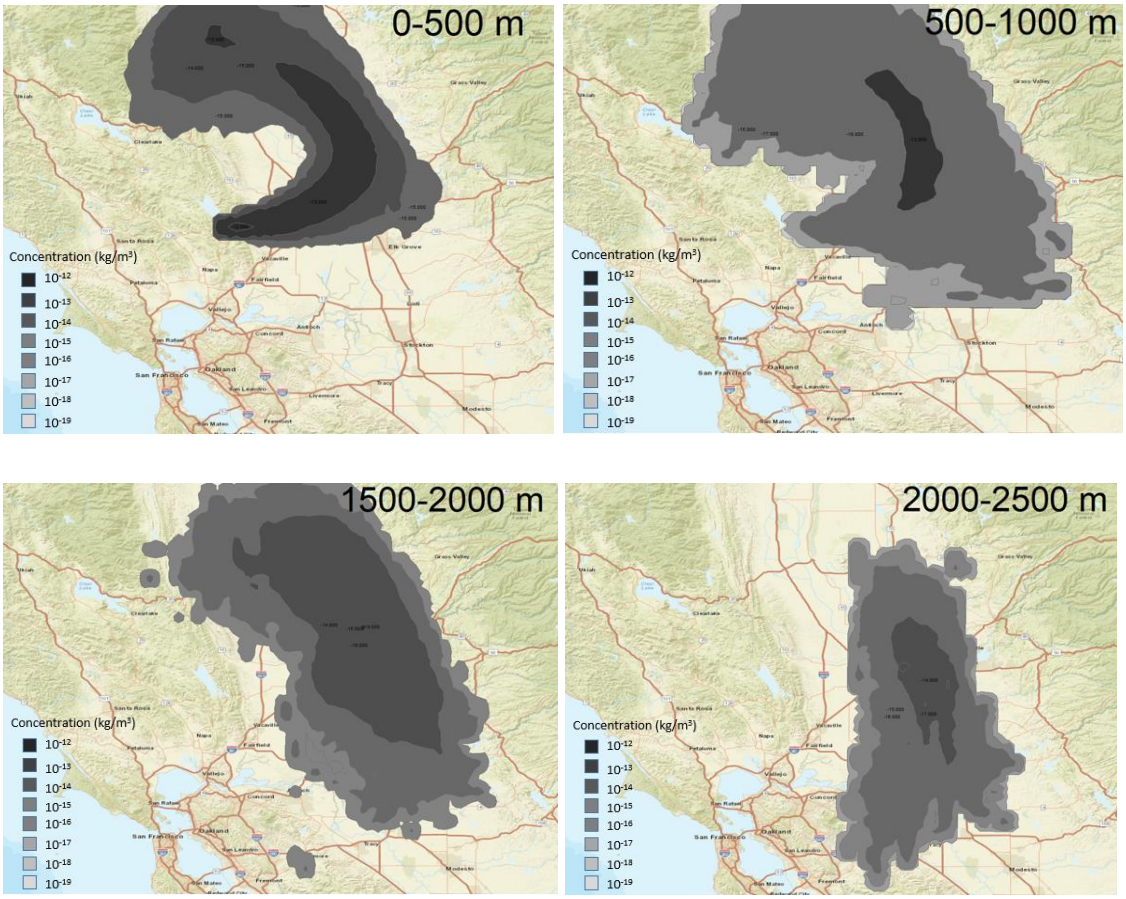

Figure 7: Map showing influence of County fire plume from July 3, as modeled by HYSPLIT. The figure is a vertical integration of particles from 0 to 500 m (top left) and 500 to 1000 m (top right) 1500 to 2000 (bottom left) and 2000 to 2500 (bottom right).

As shown in Table 1, BC particle size is a function of its source. Therefore, the size of a particle may give insights into where it came from. This is demonstrated by splitting apart RF 11 and analyzing sections separately. North of the fire a high concentration of particles existed that

are larger on average than those from the remainder of the flight. A mono-modal log-normal curve was fit to the size distribution to estimate mass mean diameter (MMD) of the particles (Figure 8). The curve was fit to the size distribution between 90 and 425 nm; larger sizes were excluded from the fit in order to avoid issues with counting statistics and detector overlap (Dahlkötter et al., 2014). The concentration of BC at this interval was 11.8 μg/m^3, an order of magnitude higher than the flight average. The MMD of the particles in the plume is 181 nm, the distribution of which is shown in Figure 8. This MMD is similar to those reported in other studies of particles generated under similar circumstances, as shown in Table 1 (Kondo et al., 2011; May et al., 2014b; Pratt et al., 2011; Sahu et al., 2012).

Another size distribution from RF 11 is presented in Figure 8. This distribution is calculated in the same manner, using data between soundings #3 and #4, which occurred over the San Francisco Bay area at an altitude of approximately 1200 m. According to the HYSPLIT data shown in Figure 7, this area received no influence from the fire. The average concentration of BC was 1.59 μg/m^3 over this interval. This size distribution had an MMD of 143 nm, closer to the distributions of BB emissions scavenged by wet deposition (unlikely, given lack of precipitation), or urban emissions (Metcalf et al., 2012; Schwarz et al., 2008; Taylor et al., 2014). Based on proximity to a major metropolitan area, BC size distribution, and the HYSPLIT model, it is apparent that this air mass contained strong influence from urban emissions and minimal influence from the fire burning 50 miles downwind.

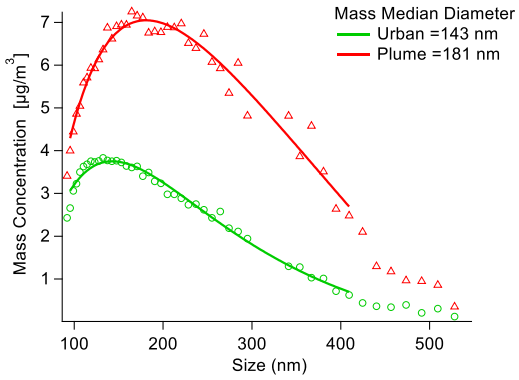

Figure 8: Size distribution of BC in the plume (purple), out of the plume (blue), and the plume without urban influence (red).

RF 11 sampled at an average altitude of 1150 m. The flight deviated from this average to capture four vertical corkscrew flight patterns called soundings to determine the vertical distribution of the plume. Each sounding provides information on maximum mixing depth and any temperature inversion layers. Sounding 3 (shown in Figure 6) was approximately 15 miles away from the fire origin, near the city of Vacaville, CA. Due to the proximity to the fire, this sounding can characterize the fire-influenced air mass. Sounding 4 (also shown in Figure 6) was over the over the Pacific Ocean, approximately 80 miles from the fire origin; this sounding was represents a background sample of the clean marine environment. The direction of travel

between these two soundings is southeast, following a visible plume. The age of sampled particles is difficult to estimate due to the wind direction and complex topography of the area. Sounding #3 features a well-mixed vertical distribution of BC from ground level up to the maximum mixing depth of 2000 m. The mass concentration of BC remains constant near 1 $\mu g/m^3$ for both soundings. The mixing depth is identified on the left side of Figure 9 by a sharp drop in dew point. The BC in sounding #3 comes from a variety of sources including the County fire and the city of Vacaville. Sounding #4 shows a confined layer of increased BC concentration between the inversion layer at 700 m and the upper bounds of the mixing layer at approximately 1400 m. This sounding likely contains little influence from the fire 80 miles upwind and is therefore represents primarily urban emissions from San Francisco and offshore shipping.

Figure 9: *left:* Vertical profile of meteorological conditions during two soundings. *Right:* BC concentration during the two soundings.

To characterize the origins of BC, it is important to measure chemical composition of non-refractory aerosol as well as refractory BC to characterize the total air mass and distinguish

among combustion sources. For example, sulfate can approach ~20% by mass of aerosol in fossil fuel-dominated plumes (Akagi et al., 2011; Merlet & Andreae, 2001), while comprising 3-8% of mass in plumes dominated by biomass burning (Kondo et al., 2011; Sahu et al., 2012). Figure 10 demonstrates the absence of sulfate and high concentration of organic particles and BC, which indicates an air mass dominated by biomass burning. Within BB plumes, high concentration of organic aerosol also indicates a smoldering combustion, whereas high BC is indicative of flaming combustion (Kondo et al., 2011; McMeeking et al., 2009). Elevated BC and organic fractions throughout RF 11 corroborate the HYSPLIT results, that nearly the entire flight path was affected by the fire.

At approximately 2:50 PM, the plane entered the plume on the north side of the fire where the BC concentration was highest. At this point, the BC concentration was significantly elevated (5 times the flight average) for 3 minutes and the plume was approximately 9 km wide. Plume crossing at this point was used to generate the size distribution on the left side of Figure 8. This plume crossing coincides with a jump in BC fraction that is not seen in total aerosol mass. Within this plume, BC constituted 49% of the total aerosol mass.

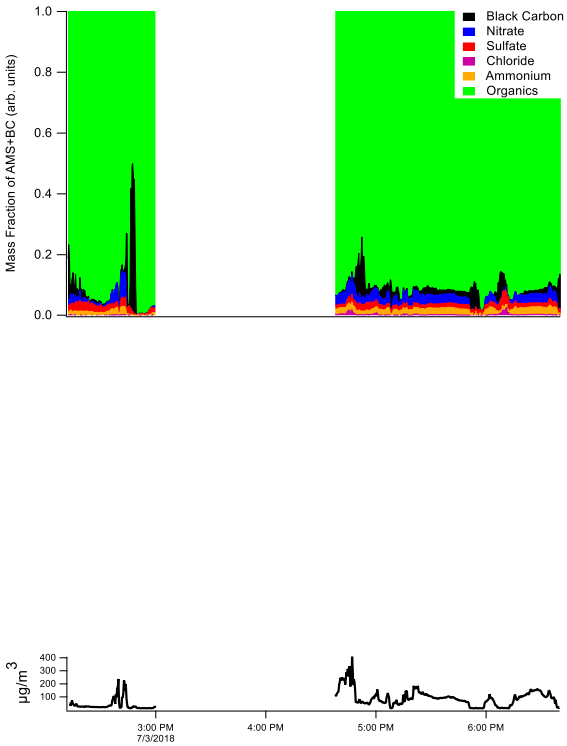

Figure 10: RF 11 chemical composition (top) and concentration of aerosols < 1 µm (bottom) as measured by AMS + SP2. The gap in the middle represents a refueling stop in Santa Rosa.

The County Fire had burned more than 90,000 acres before our sampling on July 3. The results from this sampling indicate that the fire produced significantly different BC particle MMD in the plume (177 nm) and out of the plume (141 nm), even though the entire area was influenced by the fire according to AMS and HYSPLIT criteria. Soundings #3 and #4 demonstrate BC mixing up until, but not past, maximum mixing depths of 2100 m and 1400 m, respectively. The AMS data display high organic aerosol loading, even higher than other BB sources reported

elsewhere in literature (Sahu et al., 2012). The AMS+SP2 also indicates a spike in BC mass as high as 49% of total ultrafine aerosol in the direct line of the fire plume.

Pawnee and Diablo Fires

Research flights 6 and 8 were intended to sample emissions from the Pawnee Fire, a smaller 15,000 acre fire near Clearlake, CA. The objective was to characterize the air mass inside and outside the fire plume. However, the signal from the Pawnee Fire was insufficiently strong to significantly influence the air mass during either flight. California's Sacramento Valley has a significant background concentration of BC due to nearly continuous wildfires during fire season, agriculture, and urban emissions (Watson et al., 2006; Zhang et al., 2016). Thus, RF 6 and RF 8 provide a characterization of the Sacramento Valley, allowing establishment of background BC concentrations for the well mixed Sacramento valley during the fire season. The flight pattern for each flight is similar and are displayed in Figure 11 and Figure 12 colored by BC mass concentration. The Twin Otter transited north from Marina Municipal Airport to the Sacramento Valley, north east of Sacramento. From here, the Twin Otter flew east-west grid patterns up the valley, getting as close to the total flight restriction zone as possible before completing downwind and upwind vertical soundings. RF 6 also included a refueling stop in Santa Rosa before returning to the fire for more sampling.

The Pawnee Fire was active from June 23 until July 2, 2018 between Clear Lake and Indian Valley Reservoir. The flora in that area includes blue oaks, California laurel, foothill pine, California buckeye, and mountain mahogany, for which the fuel is very similar to that of the County Fire described above. Unlike the County Fire, the winds during the two sampling days of the Pawnee Fire were coming out of the north, pushing smoke towards the east and south.

A third fire, the Diablo Fire, was also captured on RF8 and shown in Figure 11. This freshly ignited fire was the dominant feature in the air mass it affected, but the data collected are limited to one vertical sounding (which does not include data from the AMS). The plume from the Diablo fire exhibited an average mass concentration of 1.67 $\mu g/m^3$ BC, compared to 0.045 $\mu g/m^3$ in the surrounding area. This high particle loading displayed a much lower MMD (116 nm) than that seen anywhere else in this field campaign. The reason for the low MMD remains unknown. Figure 11 only shows one area of high concentration from this fire because it was not active until the final return trip past this location.

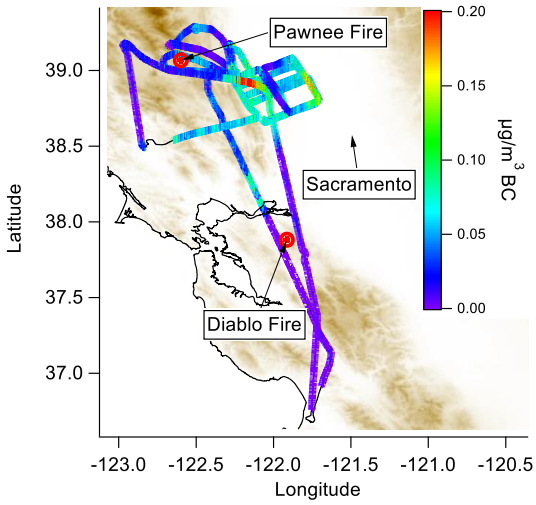

Figure 11: Flight tracks of RF 6, which occurred on June 28th, colored by BC concentration.

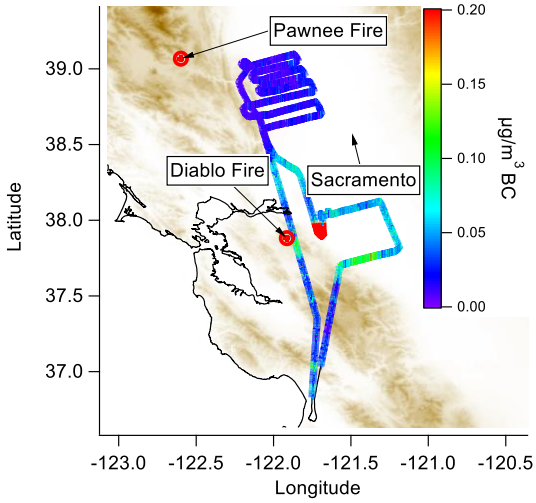

Figure 12: Flight tracks of RF 8, which occurred on June 29th, colored by BC concentration. The sole hot spot is due to an accidental sampling of the Mt. Diablo Fire shortly after its ignition. Thin black lines indicate the flight track while the SP2 was off.

Size distributions are displayed in Figure 13 for the entire flight for RF 8 (excluding the Diablo Fire), and the Diablo fire. The proximity to the recently ignited Diablo Fire presented a rare opportunity to compare the same area on the same day before and during a fire event. The addition of a strong influence from the fresh Diablo Fire produces a notable shift upwards in MMD from 153 nm to 181 nm, as shown in Figure 13. The urban background BC concentration is

low for the duration of RF 8, so the Diablo fire plume is entirely fire-generated particles. The BC size distribution in the Diablo Fire plume (176 nm) is very similar to that in the County Fire plume (181 nm) shown in Figure 8.

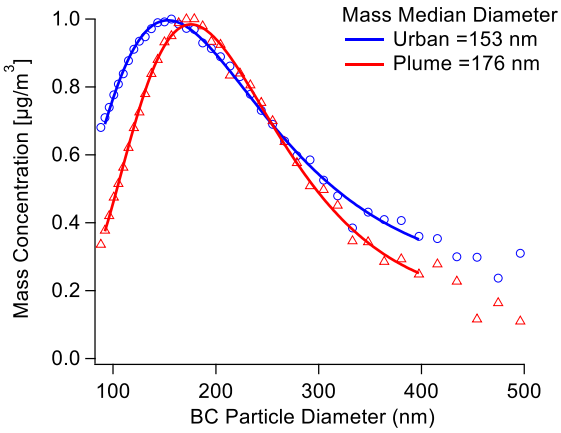

Figure 13: Size distribution of BC particles from RF 8 excluding the Diablo Fire, and the Diablo fire. The signal peaks have individually been normalized to 1.

AMS data from RF 6 (Figure 14) are very similar to other long term sampling campaigns in the SV (Moore et al., 2012; Setyan et al., 2012). Each major species is within 5% of the average values measured during the CARES (Setyan et al., 2012) and CALNEX (Moore et al.,

2012) campaigns which spanned from May 4 to June 28, 2010. The most notable difference is in sulfate, which occupies 10 and 11% of total aerosol mass in summer 2010, but 15% in RF 6. Based on these similarities, RF 6 will be used as a normal background aerosol for the remaining analysis.

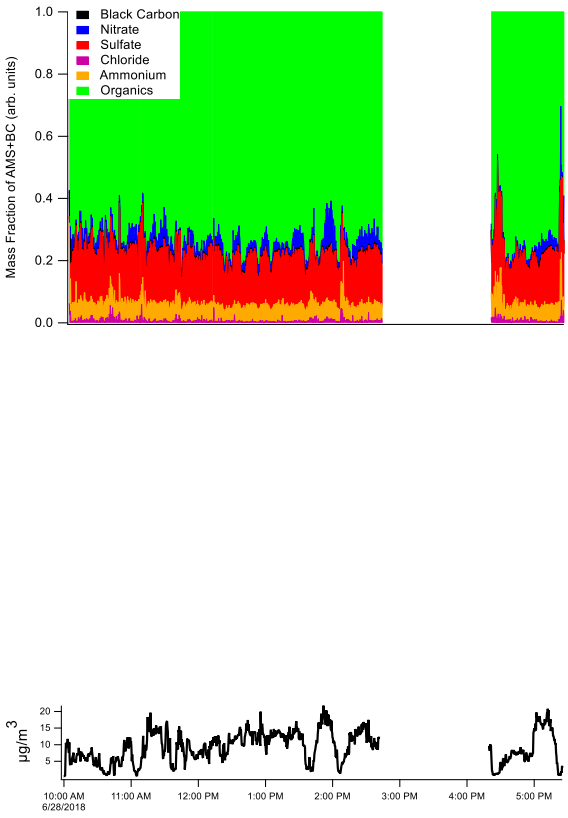

Figure 14: RF 6 chemical composition (top) and concentration of aerosols < 1 µm (bottom) as measured by AMS + SP2. The gap in the middle represents a refueling stop in Santa Rosa.

The AMS data from RF 6 (Figure 14) is starkly different from that of RF 11 (Figure 10) and several differences should be noted. The first being the quantity of aerosol- RF 11 exceeds 200 $\mu g/m^3$ 6 times, while RF 6 never exceeds 20 $\mu g/m^3$. The increase in mass is not uniform across all species, it mostly comes from an increase in organics, which jump from an average of 5.6 $\mu g/m^3$ in RF 6 to 57.9 $\mu g/m^3$ in RF 11. Nitrates also increase by an order of magnitude by mass while sulfate and ammonia remain relatively constant and chloride even slightly decreases. Average BC mass also increased from 0.041 $\mu g/m^3$ in RF 6 to 1.30 $\mu g/m^3$ in RF 11. Each of these relative differences is summarized in Table 5.

These statistics strengthen the claim that RF 11 is fire influenced when compared to RF 6. Sulfate is a tracer for fossil fuel combustion because sulfur is found in higher quantities in liquid and solid fossil fuels than in biomass vegetation (Akagi et al., 2011; Merlet & Andreae, 2001). Because the fires have no effect on fossil fuel combustion, the concentration of sulfate does not change significantly between the two days. Neither RF 6 nor RF 11 occurred over a weekend, eliminating the possibility of influence of the weekend effect (Metcalf et al., 2012); however, RF 11 did occur on July 3rd, the day prior to a major US holiday. Holiday traffic has the potential to increase fossil fuel combustion and therefore sulfate concentration, but this effect appears insignificant. McMeeking et al. (2009) does show that the chaparral and oak fuels present in the County Fire generate sulfate, but as shown in Table 5, this is not reflected in measurements. This fuel type also generates large quantities of organics and BC, which supports the large increase in these two species between days. RF 8, which contains the Diablo Fire, is not presented here.

Experiments have been performed in a laboratory setting to determine the amount of each species measured by the AMS emitted per quantity of fuel, referred to as emission factors (EF). EF are useful when estimating the quantity of a species released to the atmosphere from a fire of known fuel type. EF measured during the FLAME experiments (Chen et al., 2007; Hays et al., 2002; McMeeking et al., 2009) include the fuel types burned in the Pawnee and County Fires, and therefore allow for a prediction of aerosol speciation from these events. The composition analysis in FLAME extends up to 2.5 µm and includes combustion variables such as flaming/smoldering combustion and water content, while MACAWS data is limited to 1 µm upper cut size (AMS limit) and limited information on combustion. Appropriate EF from McMeeking et al. (2009) will be used to predict plume composition.

Table 3: Emission factors are reported in g species kg^{-1} dry fuel, except that BC and OC are g C kg^{-1} dry fuel. Adapted from (Chen et al., 2007; Hays et al., 2002; McMeeking et al., 2009).

Group	**BC**	**OC**	**NH_4^+**	**Cl^-**	**NO_3^-**	**SO_4^{2-}**
Chaparral	0.5 ± 0.4	6.6 ± 10.1	0	0.2 ± 0.1	0.1± 0.1	0.2± 0.1
Oak	0.4	10.6	0.1	0.15	0.36	0.12
Fuel	0.45 ± 0.4	8.6 ±10.1	0.05	0.18 ± 0.1	0.23 ± 0.1	0.16 ± 0.1

Influence predicted by McMeeking et al. (2009) is based fuel type on descriptions and images of flora from the burned area before the fire. A 50/50 split of chaparral and Oak has been used to represent the fuel type (Berryessa Management Plan). Because total mass of fuel burned is difficult to estimate, and upwind transportation of aerosol is even more difficult, the

aerosol generation has been normalized to grams of each species per gram of BC found in RF 11. The math used to generate these predictions listed in Table 5 is described in Table 4. RF 11 prediction is calculated by adding the actual RF 6 data to the influence predicted by McMeeking et al. (2009). The quantity of each species detected by the AMS+SP2 present will change based on proximity to fire, time since emission, and transport phenomenon. However, in the absence of additional major sources, the relative abundance of each species to other species will not change. The residual is then calculated by subtracting the actual RF 11 data from the predicted data. The calculation leaves a significant residual, which is assumed to be a difference in background between RF 6 and 11. Some of the residual can be attributed to instrument error (Table 2), uncertainty in fuel composition, and uncertainty in emission factors (shown as ± in the RF 11 prediction column). The under prediction of organics agrees with Sahu et al. (2012), who expect a lower measured mass fraction of organics.

Table 4: Calculations for Table 5.

Species *i*	**Abbreviation**	**Calculation**
Background Mass	$M_{i,bg}$	Measured
Emission Factor	EF_i	Literature
Predicted Influence from County Fire	$M_{i,inf}$	$EF_i \times \frac{M_{BC,\,meas}}{EF_{BC}}$
Predicted Plume	$M_{i,pred}$	$M_{i,inf} + M_{i,bg}$

Table 5: Change in aerosol speciation in the Sacramento Valley between a normal day (RF 6) and one with fire influence (RF 11).

Species	Background (Measured) ($\mu g/m^3$)	Fuel Emission Factors (g/kg_{fuel})	Influence Predicted by Literature ($\mu g/m^3$)	County Fire (Prediction) ($\mu g/m^3$)	County Fire (Measured) ($\mu g/m^3$)	Difference (%)
BC	0.04	0.45 ± 0.4	1.26	1.3 ± 1.12	1.3	--
Org.	5.62	8.6 ±10.1	23.24	28.9 ± 28.3	57.83	50
SO_4^{2-}	1.19	0.05	0.448	1.64 ± 0.28	1.09	-50
NO_3^-	0.28	0.18 ± 0.1	0.644	0.92 ± 0.28	1.87	51
NH_4^+	0.4	0.23 ± 0.1	0.14	0.54	1.17	54
Cl^-	0.05	0.16 ± 0.1	0.504	0.55 ± 0.28	0.28	-96

Conclusions

In this document, several characteristics of atmospheric black carbon are presented as measured during the MACAWS field campaign. A background concentration of BC and other aerosol species was first established to provide context for fire event measurements. This background concentration lies within 5% of that measured during other studies (Moore et al., 2012; Setyan et al., 2012; Watson et al., 2006; Zhang et al., 2016) in the Sacramento Valley, and includes a BC size distribution centered around 153 nm, BC loading of 0.045 $\mu m/m^3$, and a variety of other aerosols composed of approximately 75% organics, 15% sulfate, and the remainder ammonia, chlorides, and nitrates. Several fires were examined of varying size and during various atmospheric conditions. The larger and more active Pawnee Fire dominated the air mass, raising BC concentration to 11.8 $\mu g/m^3$ and organics to 92%, overpowering the background influence from fossil fuels. Meanwhile, the smaller and less active County Fire failed to significantly alter the air mass in the surrounding area. Due to the frequency of such fires in the Sacramento Valley in the summer, it represented a portion of the "typical" background. Finally, a much smaller Diablo Fire was sampled in close proximity immediately after ignition. Despite the close proximity sampling of this fresh fire, it displayed a lower mass loading and smaller median diameter than the older, more dilute Pawnee Fire, raising questions about the changing characteristics of emitted particles over the lifetime of a fire.

Using BC data from the Pawnee Fire and emission factors from the FLAME studies (McMeeking et al., 2009), the relative abundance of refractory aerosol was predicted. These predicted constituents were compared to measured values to extract the residual between measured and predicted. This residual varied in relative magnitude and is the result of additional

influence and measurement error. This was an important attempt to use a single BC measurement to infer the presence of other species.

Black carbon is of utmost importance for climate, human health, and the thermodynamic structure of the atmosphere. The impact has the potential to increase in coming decades as wildfires increase in intensity and frequency along the Sacramento Valley. This research adds to the scientific community's understanding of the quantity and characteristics of atmospheric BC emitted from these wildfires.

Evaluations

Assessment of Research Objectives

As stated in the research overview, the purpose of this work was to increase overall understanding of ultrafine emissions from wildfires, especially black carbon particles. In order to contribute to this broader topic, the specific objectives addressed here are:

- Determine background mass concentrations of black carbon and other non-refractory species in the Sacramento Valley during fire season
- Investigate the size distribution of black carbon aerosol from wildfires
- Examine the emission of co-emitted aerosol from wildfires
- To use models and on board instruments to examine the plume dynamics in the atmosphere

Although several studies have already investigated background loading in the Sacramento Valley and examined size distributions of BC from wildfires, the diversity of sources necessitates additional research. Emissions from urban and industrial sources evolve over time with improving technology and changing regulations. The dynamic nature of this change requires that background concentration be investigated during each field campaign, rather than relying on published values from a decade prior. Similarly, each wildfire is different than the last. Many variables including combustion phase, efficiency, temperature, fuel type, and atmospheric conditions contribute to particle size distribution and mass concentration of BC and co-emitted aerosols. This investigation contributes to existing data found in literature.

Knowledge gaps were filled in the process of investigating the emission of co-emitted aerosols by comparing published emission factors to measured values. Although this technique

is in its infancy, if developed further, could have significant implications for climate modeling. The technique allows scientists to measure one species of aerosol and estimate all remaining species. Potential applications include global remote sensing and reduced payload on future aircraft-based campaigns. Potential outcomes include improved estimations of aerosol emissions from wildfires, leading to improved accuracy of data for climate models.

Although modeling an emission source as done here with the County Fire is not a new technique, it does have implications for public health. Improved plume modelling allows policy makers to be better informed about the potential impacts of a fire. With knowledge of these impacts (e.g. it is estimated that the fire will increase $PM_{2.5}$ concentrations to 100 $\mu g/m^3$ for the next 12 hours across the city) policy makers are better informed of impacts and can develop better fire management procedures. The County Fire is a prime example of this; the majority of the plume was transported away from the city of Sacramento, putting few people in danger. The 2,500 firefighters involved could have been deployed to other fires that would directly affect major metropolitan areas.

The field has several options on how it can expand on this work. Comparing emission factors to measured concentrations should be the focus of additional field work in order to build a relationship between the two. Additionally, the discrepancies between measured and modeled plume should be investigated to determine if changes need to be made to the model. The information provided here about background concentration and size distribution can be incorporated into climate models to investigate the climate effects of BC.

Recommended Future Work

There are also numerous opportunities for the Clemson Air Quality Lab to expand upon the work done here. Of the 16 total research flights, 13 are yet to be analyzed, including all the ship tracking flights. The data for these flights has been loaded into Igor and left for a future student. The most attractive of these flights are 7, 12, 13, and 15, which each present an excellent ship tracking case study. Analysis of this data could be compares to lab studies of ship emissions (Corbin et al., 2018), and an attempt can be made to generate a model to improve characterization of BC emitted from shipping channels.

Additionally, the Clemson Air Quality Lab could begin to examine the mixing state of BC, using information available from the split detectors in addition to scattering instruments such as the Particle Soot Absorption Photometer (PSAP) and collaborative measurements with Geoffrey Smith to extract information on BC coating. Collaboration with Dr. Smith would allow a more complete description of atmospheric BC and help to answer important questions about the particles' light absorption and radiative forcing. Significant hurdles would have to be overcome in instrumentation and analysis before this type of work would be possible.

Although the CEF deployment did not occur this year, it likely will in future years. Because this lab will be in close proximity to the controlled burns for many years to come, and the emissions from those burns are unlikely to change appreciably from year to year, a unique opportunity exists here as well. The SP2 can be calibrated in the field, using the particles of interest. Such calibration can be achieved by running a series of instruments in line that Clemson already owns. The result is a heated atmospheric aerosol sample of known mass being fed into the SP2 as a calibrant. This technique is uncommon due to practical limitations but represents

the best possible calibration for the SP2. It would allow for future CEF sampling to use an on-site calibration curve, which could be the crowning achievement of a paper devoted to SP2 calibration, expanding on Laborde et al. (2012).

References

Akagi, S. K., Yokelson, R. J., Wiedinmyer, C., Alvarado, M. J., Reid, J. S., Karl, T., et al. (2011). Emission factors for open and domestic biomass burning for use in atmospheric models. *Atmospheric Chemistry and Physics*, *11*(9), 4039–4072. https://doi.org/10.5194/acp-11-4039-2011

Anderson, T. L., Covert, D. S., Marshall, S. F., Laucks, M. L., Charlson, R. J., Waggoner, A. P., et al. (1996). Performance characteristics of a high-sensitivity, three-wavelength, total scatter/backscatter nephelometer. *Journal of Atmospheric and Oceanic Technology*. https://doi.org/10.1175/1520-0426(1996)013<0967:PCOAHS>2.0.CO;2

Archer, D., Eby, M., Brovkin, V., Ridgwell, A., Cao, L., Mikolajewicz, U., et al. (2009). Atmospheric Lifetime of Fossil Fuel Carbon Dioxide. *Annual Review of Earth and Planetary Sciences*, *37*(1), 117–134. https://doi.org/10.1146/annurev.earth.031208.100206

Arnott, W. P., Walker, J. W., Moosmüller, H., Elleman, R. A., Jonsson, H. H., Buzorius, G., et al. (2006). Photoacoustic insight for aerosol light absorption aloft from meteorological aircraft and comparison with particle soot absorption photometer measurements: DOE Southern Great Plains climate research facility and the coastal stratocumulus imposed perturbat. *Journal of Geophysical Research Atmospheres*, *111*(5), 1–16. https://doi.org/10.1029/2005JD005964

Barath, S., Mills, N. L., Lundbäck, M., Törnqvist, H., Lucking, A. J., Langrish, J. P., et al. (2010). Impaired vascular function after exposure to diesel exhaust generated at urban transient running conditions. *Particle and Fibre Toxicology*, *7*, 1–11. https://doi.org/10.1186/1743-8977-7-19

Baumgardner, D., Kok, G., & Raga, G. (2004). Warming of the Arctic lower stratosphere by light absorbing particles. *Geophysical Research Letters*, *31*(6), n/a-n/a. https://doi.org/10.1029/2003gl018883

Bond, T. C., & Bergstrom, R. W. (2006). Light absorption by carbonaceous particles: An investigative review. *Aerosol Science and Technology*, *40*(1), 27–67. https://doi.org/10.1080/02786820500421521

Bond, T. C., Anderson, T. L., & Campbell, D. (1999). Calibration and Intercomparison of Filter-Based Measurements of Visible Light Absorption by Aerosols. *Aerosol Science and Technology*, *30*(6), 582–600. https://doi.org/10.1080/027868299304435

Bond, T. C., Streets, D. G., Yarber, K. F., Nelson, S. M., Woo, J. H., & Klimont, Z. (2004). A technology-based global inventory of black and organic carbon emissions from combustion. *Journal of Geophysical Research: Atmospheres*, *109*(14), 1–43. https://doi.org/10.1029/2003JD003697

Bond, T. C., Doherty, S. J., Fahey, D. W., Forster, P. M., Berntsen, T., Deangelo, B. J., et al. (2013). Bounding the role of black carbon in the climate system: A scientific assessment. *Journal of Geophysical Research Atmospheres*, *118*(11), 5380–5552. https://doi.org/10.1002/jgrd.50171

Boucher, O., Randall, D., Artaxo, P., Bretherton, C., & Feingold, G. (2013). *Clouds and Aerosols*-

IPCC AR5.

CalFire. (2019). Stats and Events. Retrieved from https://fire.ca.gov/stats-events/

Chen, L. W. A., Moosmüller, H., Arnott, W. P., Chow, J. C., Watson, J. G., Susott, R. A., et al. (2007). Emissions from laboratory combustion of wildland fuels: Emission factors and source profiles. *Environmental Science and Technology*, *41*(12), 4317–4325. https://doi.org/10.1021/es062364i

Clarke, A. D., Shinozuka, Y., Kapustin, V. N., Howell, S., Huebert, B., Doherty, S., et al. (2004). Size distributions and mixtures of dust and black carbon aerosol in Asian outflow: Physiochemistry and optical properties. *Journal of Geophysical Research D: Atmospheres*, *109*(15), 1–20. https://doi.org/10.1029/2003JD004378

Corbin, J. C., Pieber, S. M., Czech, H., Zanatta, M., Jakobi, G., Massabò, D., et al. (2018). Brown and black carbon emitted by a ship engine operated on heavy fuel oil and distillate fuels: optical properties, size distributions, emission factors. *(Under Review)*, (October). https://doi.org/10.1029/2017JD027818

Dahlkötter, F., Gysel, M., Sauer, D., Minikin, A., Baumann, R., Seifert, P., et al. (2014). The Pagami Creek smoke plume after long-range transport to the upper troposphere over Europe – Aerosol properties and black carbon mixing state. *Atmospheric Chemistry and Physics*, *14*(12). https://doi.org/10.5194/acp-14-6111-2014

DeCarlo, P. F., Dunlea, E. J., Kimmel, J. R., Aiken, A. C., Sueper, D., Crounse, J., et al. (2008). Fast airborne aerosol size and chemistry measurements above Mexico City and Central Mexico during the MILAGRO campaign. *Atmospheric Chemistry and Physics*, *8*(14), 4027–4048. https://doi.org/10.5194/acp-8-4027-2008

DeCarlo, Peter F., Kimmel, J. R., Trimborn, A., Northway, M. J., Jayne, J. T., Aiken, A. C., et al. (2006). Field-deployable, high-resolution, time-of-flight aerosol mass spectrometer. *Analytical Chemistry*, *78*(24), 8281–8289. https://doi.org/10.1021/ac061249n

Demuzere, M., Trigo, R. M., De Arellano, J. V. G., & Van Lipzig, N. P. M. (2009). The impact of weather and atmospheric circulation on O3 and PM10 levels at a rural mid-latitude site. *Atmospheric Chemistry and Physics*, *9*(8), 2695–2714. https://doi.org/10.5194/acp-9-2695-2009

Fawole, O. G., Cai, X. M., & Mackenzie, A. R. (2016). Gas flaring and resultant air pollution: A review focusing on black carbon. *Environmental Pollution*, *216*, 182–197. https://doi.org/10.1016/j.envpol.2016.05.075

Feng, Y., Chen, Y., Guo, H., Zhi, G., Xiong, S., Li, J., et al. (2009). Characteristics of organic and elemental carbon in PM2.5samples in Shanghai, China. *Atmospheric Research*, *92*(4), 434–442. https://doi.org/10.1016/j.atmosres.2009.01.003

Final Management Plan for the Lake Berryessa Wildlife Area. (1998). Retrieved from https://www.usbr.gov/mp/ccao/berryessa/vsp/docs-forms/10-08-03-lake-berryessa-wildlife-area.pdf

Fried, J. S., Torn, M. S., & Mills, E. (n.d.). Uncorrected Proof the Impact of Climate Change on Wildfire Severity : a Regional Forecast for Northern California, (5143859), 1–23.

Gertler, C. G., Puppala, S. P., Panday, A., Stumm, D., & Shea, J. (2016). Black carbon and the Himalayan cryosphere: A review. *Atmospheric Environment*, *125*, 404–417. https://doi.org/10.1016/j.atmosenv.2015.08.078

Harrison, R. M., & Yin, J. (2000). Particulate matter in the atmosphere: which particle properties are important for its effects on health? https://doi.org/10.1016/S0048-9697(99)00513-6

Hays, M. D., Geron, C. D., Linna, K. J., Smith, N. D., & Schauer, J. J. (2002). Speciation of gas-phase and fine particle emissions from burning of foliar fuels. *Environmental Science and Technology*, *36*(11), 2281–2295. https://doi.org/10.1021/es0111683

Hegg, D. A., Covert, D. S., Jonsson, H., & Covert, P. A. (2005). Determination of the transmission efficiency of an aircraft aerosol inlet. *Aerosol Science and Technology*, *39*(10), 966–971. https://doi.org/10.1080/02786820500377814

Highwood, E. J., & Kinnersley, R. P. (2006). When smoke gets in our eyes: The multiple impacts of atmospheric black carbon on climate, air quality and health. *Environment International*, *32*(4), 560–566. https://doi.org/10.1016/j.envint.2005.12.003

Janssen, N. A. H., Gerlofs-Nijland, M., Lanki, T., Salonen, R., Cassee, F., Hoek, G., et al. (2012). Health Effects of Black Carbon. https://doi.org/10.1016/j.atmosenv.2007.03.042

Kennedy, I. M. (2007). The health effects of combustion-generated aerosols. *Proceedings of the Combustion Institute*, *31 II*, 2757–2770. https://doi.org/10.1016/j.proci.2006.08.116

Kleefeld, S., Hoffer, A., Krivácsy, Z., & Jennings, S. G. (2002). Importance of organic and black carbon in atmospheric aerosols at Mace Head, on the West Coast of Ireland (53°19'N, 9°54'W). *Atmospheric Environment*, *36*(28), 4479–4490. https://doi.org/10.1016/S1352-2310(02)00346-1

Kondo, Y., Matsui, H., Moteki, N., Sahu, L., Takegawa, N., Kajino, M., et al. (2011). Emissions of black carbon, organic, and inorganic aerosols from biomass burning in North America and Asia in 2008. *Journal of Geophysical Research Atmospheres*, *116*(8), 1–25. https://doi.org/10.1029/2010JD015152

Laborde, M., Mertes, P., Zieger, P., Dommen, J., Baltensperger, U., & Gysel, M. (2012). Sensitivity of the Single Particle Soot Photometer to different black carbon types. *Atmospheric Measurement Techniques*, *5*(5), 1031–1043. https://doi.org/10.5194/amt-5-1031-2012

Lu, G., Brook, J. R., Rami Alfarra, M., Anlauf, K., Richard Leaitch, W., Sharma, S., et al. (2006). Identification and characterization of inland ship plumes over Vancouver, BC. *Atmospheric Environment*, *40*(15), 2767–2782. https://doi.org/10.1016/j.atmosenv.2005.12.054

May, A. A., McMeeking, G. R., Lee, T., Taylor, J. W., Craven, J. S., Burling, I., et al. (2014a). Aerosol emissions from prescribed fires in the United States: A synthesis of laboratory and aircraft measurements. *Journal of Geophysical Research*, *119*(20), 11826–11849. https://doi.org/10.1002/2014JD021848

May, A. A., McMeeking, G. R., Lee, T., Taylor, J. W., Craven, J. S., Burling, I., et al. (2014b). Aerosol emissions from prescribed fires in the United States: A synthesis of laboratory and aircraft measurements. *Journal of Geophysical Research*, *119*(20). https://doi.org/10.1002/2014JD021848

McConnell, J. R., Edwards, R., Kok, G. L., Flanner, M. G., Zender, C. S., Saltzman, E. S., et al. (2007). 20th-Century Industrial Black Carbon Emissions Altered Arctic Climate Forcing. *Science*, *317*(September), 1381–1385.

McMeeking, G. R., Kreidenweis, S. M., Baker, S., Carrico, C. M., Chow, J. C., Collett, J. L., et al. (2009). Emissions of trace gases and aerosols during the open combustion of biomass in the laboratory. *Journal of Geophysical Research Atmospheres*, *114*(19), 1–20. https://doi.org/10.1029/2009JD011836

Merlet, P., & Andreae, M. O. (2001). Emission of Trace Gases and Aerosols from Biomass Burning. *Atmospheric Chemistry and Physics*, *11*(3), 1141–1165. https://doi.org/10.5194/acp-11-4039-2011

Metcalf, A. R., Craven, J. S., Ensberg, J. J., Brioude, J., Angevine, W., Sorooshian, A., et al. (2012). Black carbon aerosol over the Los Angeles Basin during CalNex. *Journal of Geophysical Research Atmospheres*, *117*(8), 1–24. https://doi.org/10.1029/2011JD017255

Middlebrook, A. M., Bahreini, R., Jimenez, J. L., & Canagaratna, M. R. (2012). Evaluation of composition-dependent collection efficiencies for the Aerodyne aerosol mass spectrometer using field data. *Aerosol Science and Technology*, *46*(3), 258–271. https://doi.org/10.1080/02786826.2011.620041

Mills, N. L., Robinson, S. D., Fokkens, P. H. B., Leseman, D. L. A. C., Miller, M. R., Anderson, D., et al. (2008). Exposure to concentrated ambient particles does not affect vascular function in patients with coronary heart disease. *Environmental Health Perspectives*, *116*(6), 709–715. https://doi.org/10.1289/ehp.11016

Mills, N. L., Donaldson, K., Hadoke, P. W., Boon, N. A., MacNee, W., Cassee, F. R., et al. (2009). Adverse cardiovascular effects of air pollution. *Nature Clinical Practice Cardiovascular Medicine*, *6*(1), 36–44. https://doi.org/10.1038/ncpcardio1399

Moore, R. H., Cerully, K., Brock, C. A., Bahreini, R., Middlebrook, A. M., & Nenes, A. (2012). Hygroscopicity and composition of California CCN during summer 2010. *Journal of Geophysical Research: Atmospheres*, *117*(D21), n/a-n/a. https://doi.org/10.1029/2011jd017352

Moteki, N., Kondo, Y., Miyazaki, Y., Takegawa, N., Komazaki, Y., Kurata, G., et al. (2007). Evolution of mixing state of black carbon particles: Aircraft measurements over the western Pacific in March 2004. *Geophysical Research Letters*, *34*(11). https://doi.org/10.1029/2006GL028943

Moteki, N., Kondo, Y., Oshima, N., Takegawa, N., Koike, M., Kita, K., et al. (2012). Size dependence of wet removal of black carbon aerosols during transport from the boundary layer to the free troposphere. *Geophysical Research Letters*, *39*(13), 2–5. https://doi.org/10.1029/2012GL052034

Moteki, Nobuhiro, & Kondo, Y. (2010). Dependence of laser-induced incandescence on physical properties of black carbon aerosols: Measurements and theoretical interpretation. *Aerosol Science and Technology*, *44*(8), 663–675. https://doi.org/10.1080/02786826.2010.484450

Nemmar, A., Vanbilloen, H., Hoylaerts, M. F., Hoet, P. H. M., Verbruggen, A., & Nemery, B.

(2001). Passage of Intratracheally Instilled Ultrafine Particles from the Lung into the Systemic Circulation in Hamster. *About the American Journal of Respiratory and Critical Care Medicine*, *164*(9), 1665–1668. https://doi.org/10.1164/rccm2101036

Oberdörster, G., Oberdörster, E., & Oberdörster, J. (2005). Nanotoxicology: An emerging discipline evolving from studies of ultrafine particles. *Environmental Health Perspectives*, *113*(7), 823–839. https://doi.org/10.1289/ehp.7339

Penn, A., Murphy, G., Barker, S., Henk, W., & Penn, L. (2005). Combustion-derived ultrafine particles transport organic toxicants to target respiratory cells. *Environmental Health Perspectives*, *113*(8), 956–963. https://doi.org/10.1289/ehp.7661

Penner, J. E., Zhang, S. Y., & Chuang, C. C. (2003). Soot and smoke aerosol may not warm climate. *Journal of Geophysical Research: Atmospheres*, *108*(D21), 1–9. https://doi.org/10.1029/2003JD003409

Polidori, A., Kwon, J., Turpin, B. J., & Weisel, C. (2010). Source proximity and residential outdoor concentrations of PM 2.5, OC, EC, and PAHs. *Journal of Exposure Science and Environmental Epidemiology*, *20*(5), 457–468. https://doi.org/10.1038/jes.2009.39

Pratt, K. A., Murphy, S. M., Subramanian, R., Demott, P. J., Kok, G. L., Campos, T., et al. (2011). Flight-based chemical characterization of biomass burning aerosols within two prescribed burn smoke plumes. *Atmospheric Chemistry and Physics*, *11*(24), 12549–12565. https://doi.org/10.5194/acp-11-12549-2011

Regelbrugge, J. C., & Conard, S. G. (1998). Biomass and fuel characteristics of chaparral in southern California, ???

Roorda-Knape, M. C., Janssen, N. A. H., De Hartog, J. J., Van Vliet, P. H. ., Harssema, H., & Brunekreef, B. (2002). Air pollution from traffic in city districts near major motorways. *Atmospheric Environment*, *32*(11), 1921–1930. https://doi.org/10.1016/s1352-2310(97)00496-2

Sahu, L. K., Kondo, Y., Moteki, N., Takegawa, N., Zhao, Y., Cubison, M. J., et al. (2012). Emission characteristics of black carbon in anthropogenic and biomass burning plumes over California during ARCTAS-CARB 2008. *Journal of Geophysical Research Atmospheres*, *117*(16), 1–20. https://doi.org/10.1029/2011JD017401

Samset, B. H., Myhre, G., Herber, A., Kondo, Y., Li, S. M., Moteki, N., et al. (2014). Modelled black carbon radiative forcing and atmospheric lifetime in AeroCom Phase II constrained by aircraft observations. *Atmospheric Chemistry and Physics*, *14*(22), 12465–12477. https://doi.org/10.5194/acp-14-12465-2014

Schwarz, J. P., Spackman, J. R., Gao, R. S., Perring, A. E., Cross, E., Onasch, T. B., et al. (2010). The detection efficiency of the single particle soot photometer. *Aerosol Science and Technology*, *44*(8), 612–628. https://doi.org/10.1080/02786826.2010.481298

Schwarz, Joshua P., Gao, R. S., Fahey, D. W., Thomson, D. S., Watts, L. A., Wilson, J. C., et al. (2006). Single-particle measurements of midlatitude black carbon and light-scattering aerosols from the boundary layer to the lower stratosphere. *Journal of Geophysical Research Atmospheres*, *111*(16), 1–15. https://doi.org/10.1029/2006JD007076

Schwarz, Joshua P., Gao, R. S., Spackman, J. R., Watts, L. A., Thomson, D. S., Fahey, D. W., et al. (2008). Measurement of the mixing state, mass, and optical size of individual black carbon particles in urban and biomass burning emissions. *Geophysical Research Letters*, *35*(13), 1–5. https://doi.org/10.1029/2008GL033968

Sedlacek, A. J., Lewis, E. R., Kleinman, L., Xu, J., & Zhang, Q. (2012). Determination of and evidence for non-core-shell structure of particles containing black carbon using the Single-Particle Soot Photometer (SP2). *Geophysical Research Letters*, *39*(6), 2–7. https://doi.org/10.1029/2012GL050905

Setyan, A., Zhang, Q., Merkel, M., Knighton, W. B., Sun, Y., Song, C., et al. (2012). Characterization of submicron particles influenced by mixed biogenic and anthropogenic emissions using high-resolution aerosol mass spectrometry: Results from CARES. *Atmospheric Chemistry and Physics*, *12*(17), 8131–8156. https://doi.org/10.5194/acp-12-8131-2012

Sharma, S., Richard Leaitch, W., Huang, L., Veber, D., Kolonjari, F., Zhang, W., et al. (2017). An evaluation of three methods for measuring black carbon in Alert, Canada. *Atmospheric Chemistry and Physics*, *17*(24), 15225–15243. https://doi.org/10.5194/acp-17-15225-2017

Solomon, C., Balmes, J. R., Jenkins, B., & Kleinman, M. (2003). The Effect of Smoke from Burning Vegetative Residues on Airway Inflammation and Pulmonary Function in Healthy , Asthmatic , and Allergic Individuals Contract Number : 97-322, 1–61.

Stephens, M., Turner, N., & Sandberg, J. (2003). Particle identification by laser-induced incandescence in a solid-state laser cavity. *Applied Optics*, *42*(19), 3726–36. https://doi.org/10.1364/AO.42.003726

Taylor, J. W., Allan, J. D., Allen, G., Coe, H., Williams, P. I., Flynn, M. J., et al. (2014). Size-dependent wet removal of black carbon in Canadian biomass burning plumes. *Atmospheric Chemistry and Physics*, *14*(24), 13755–13771. https://doi.org/10.5194/acp-14-13755-2014

Venkatesh, R., & Somers, J. (2011). Black Carbon as a Short-Lived Climate Forcer: A Profile of Emission Sources and Co-Emitted Pollutants, *71*, 300–313. https://doi.org/10.1007/978-3-642-23825-3_27

Viswanathan, S., Eria, L., Diunugala, N., McClean, C., & Johnson, J. (2012). An Analysis of Effects of San Diego Wildfire on Ambient Air Quality. *Journal of the Air & Waste Management Association*, *56*(1), 56–67. https://doi.org/10.1080/10473289.2006.10464439

Watson, J. G., Chen, L.-W. A., Lehrman, D. E., Lowenthal, D. H., Magliano, K. A., Turkiewicz, K., & Chow, J. C. (2006). PM 2.5 chemical composition and spatiotemporal variability during the California Regional PM 10 /PM 2.5 Air Quality Study (CRPAQS) . *Journal of Geophysical Research: Atmospheres*, *111*(D10), n/a-n/a. https://doi.org/10.1029/2005jd006457

Westerling, A. L., & Bryant, B. P. (2007). Climate change and wildfire in California. *Climatic Change*, *87*(1 SUPPL). https://doi.org/10.1007/s10584-007-9363-z

Westerling, A. L., Hidalgo, H. G., Cayan, D. R., & Swetnam, T. W. (2006). Warming and earlier spring increase Western U.S. forest wildfire activity. *Science*, *313*(5789), 940–943. https://doi.org/10.1126/science.1128834

WHO. (2007). *Health Effects of Ambient Particulate Matter* (Vol. 50). https://doi.org/10.5124/jkma.2007.50.2.175

Zhang, X., Kim, H., Parworth, C. L., Young, D. E., Zhang, Q., Metcalf, A. R., & Cappa, C. D. (2016). Optical Properties of Wintertime Aerosols from Residential Wood Burning in Fresno, CA: Results from DISCOVER-AQ 2013. *Environmental Science and Technology*, *50*(4), 1681–1690. https://doi.org/10.1021/acs.est.5b04134